PROCEEDINGS OF SCIENCE

Measurement of light-by-light scattering in ultra-peripheral Pb+Pb collisions with the ATLAS detector

Mateusz Dyndal, on behalf of the ATLAS Collaboration[a,*]

[a]*AGH University of Science and Technology, Krakow, Poland*

E-mail: Mateusz.Dyndal@cern.ch

In ultra-relativistic heavy-ion collisions, one expects copious rates of $\gamma\gamma$ processes through the interaction of the large electromagnetic fields of the nuclei which can lead to light-by-light scattering via loop diagrams. This process was directly observed for the first time at the LHC by ATLAS. Final measurements of light-by-light scattering with the full Run 2 dataset with substantially reduced uncertainties are presented. This process provides a precise and unique opportunity to investigate extensions of the Standard Model such as axion-like particles.

**** The European Physical Society Conference on High Energy Physics (EPS-HEP2021), ****
**** 26-30 July 2021 ****
**** Online conference, jointly organized by Universität Hamburg and the research center DESY ****

*Speaker

PoS(EPS-HEP2021)322

1. Introduction

Light-by-light (LbyL) scattering, $\gamma\gamma \to \gamma\gamma$, is a quantum-mechanical process that is forbidden in the classical theory of electrodynamics. In the Standard Model (SM), the $\gamma\gamma \to \gamma\gamma$ reaction proceeds at one-loop level at order α_{EM}^4 (where α_{EM} is the fine-structure constant) via virtual box diagrams involving electrically charged fermions (leptons and quarks) or $W^{\pm}$ bosons (Figure 1).

The LbyL process has been proposed as a sensitive channel to study physics beyond the SM. For example, new neutral particles, such as axion-like particles (ALP), can contribute to the LbyL cross section in the form of narrow diphoton resonances [1], as shown in Figure 1. ALPs are relatively light, gauge-singlet (pseudo-)scalar particles that appear in many theories with a spontaneously broken global symmetry. Their masses and couplings to SM particles may range over many orders of magnitude.

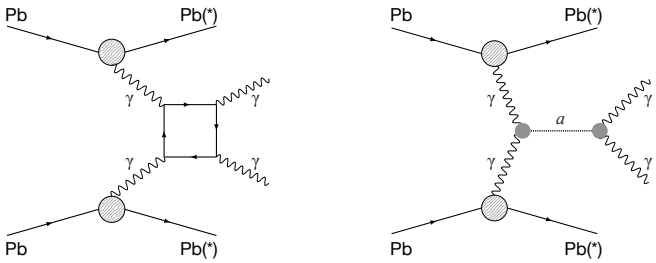

Figure 1: Schematic diagrams of (left) SM LbyL scattering and (right) axion-like particle production in Pb+Pb ultraperipheral collisions [2]. A potential electromagnetic excitation of the outgoing Pb ions is denoted by $(^*)$.

The authors of Ref. [3] proposed to measure LbyL scattering by exploiting the large photon fluxes available in heavy-ion collisions at the LHC. The first direct evidence of the LbyL process in Pb+Pb UPC at the LHC was established by the ATLAS [4, 5] and CMS [6] Collaborations, based on the 2015 Pb+Pb dataset. Exploiting a data sample of Pb+Pb collisions collected in 2018 at the same center-of-mass energy with an integrated luminosity of 1.73 nb^{-1}, the ATLAS Collaboration observed LbyL scattering with a significance of 8.2σ [7].

The new ATLAS result presents a measurement of the cross sections for Pb+Pb $(\gamma\gamma) \to$ Pb$^{(*)}$+Pb$^{(*)}$ $\gamma\gamma$ production at $\sqrt{s_{\text{NN}}} = 5.02$ TeV using a combination of Pb+Pb collision data recorded in 2015 and 2018, corresponding to an integrated luminosity of 2.2 nb^{-1} [5]. The integrated fiducial cross section and four differential distributions involving kinematic variables of the final-state photons are measured. In addition, the measured diphoton invariant mass distribution is used to set limits on ALP production via the process $\gamma\gamma \to a \to \gamma\gamma$.

2. Event selection

Candidate diphoton events were recorded using a dedicated trigger for events with moderate activity in the calorimeter but little additional activity in the entire detector. The trigger strategies for the 2015 and 2018 data sets were different.

Recorded events are required to have exactly two photons with a diphoton invariant mass ($m_{\gamma\gamma}$) greater than 5 GeV. Only photons with $E_{\mathrm{T}} > 2.5$ GeV and $|\eta| < 2.37$, excluding the calorimeter transition region $1.37 < |\eta| < 1.52$, are considered.

In order to suppress the $\gamma\gamma \to ee$ background, a veto on charged-particle tracks (with $p_{\mathrm{T}} > 100$ MeV, $|\eta| < 2.5$) is imposed. In order to reduce the background from electrons with poorly reconstructed tracks, candidate events are required to have no 'pixel tracks' in the vicinity of the photon candidate. Pixel tracks are reconstructed using only the information from the Pixel detector, and are required to have $p_{\mathrm{T}} > 50$ MeV, $|\eta| < 2.5$, and at least three hits in the Pixel detector. In order to suppress fake pixel tracks due to noise in the Pixel detector, only pixel tracks with $|\Delta\eta| < 0.5$ from the photons are considered.

To reduce other sources of fake-photon background (involving mainly calorimeter noise and cosmic-ray muons), the transverse momentum of the diphoton system is required to be below 1 GeV for $m_{\gamma\gamma} < 12$ GeV and below 2 GeV for $m_{\gamma\gamma} > 12$ GeV. To reduce real-photon background from QCD central exclusive production (CEP) $gg \to \gamma\gamma$ reactions, an additional requirement on the diphoton acoplanarity, $Aco = (1 - |\Delta\phi_{\gamma\gamma}|/\pi) < 0.01$, is used. The CEP process exhibits a significantly broader acoplanarity distribution than the $\gamma\gamma \to \gamma\gamma$ process because gluons recoil against the Pb nucleus, which then dissociates.

3. Background estimation

The $\gamma\gamma \to ee$ yield in the signal region (defined in Sec. 2) is estimated using a fully data-driven method. A control region is defined requiring exactly two photon candidates passing the signal selection, and one or two pixel tracks. The event yield observed in this control region is extrapolated to the signal region using the probability of missing the electron pixel track if the standard track is not reconstructed. The number of $\gamma\gamma \to ee$ events in the signal region is estimated to be $N_{\gamma\gamma\to ee} = 15 \pm 7$.

The CEP $gg \to \gamma\gamma$ background is estimated from MC simulation with the overall rate of this process evaluated in the $Aco > 0.01$ control region in the data. The diphoton acoplanarity distribution for events satisfying the signal region selection, but before applying the $Aco < 0.01$ requirement is shown in Figure 2. The background due to CEP in the signal region is estimated to be 12 ± 3 events.

4. Systematic uncertainties

The impact of the Level-1 trigger efficiency uncertainty on the expected signal yield is 5%. The uncertainty in the MBTS/FCal veto efficiency has negligible impact on the results.

The uncertainty in the photon reconstruction and photon particle identification (PID) efficiencies is estimated by parameterising the scale factors as a function of the photon pseudorapidity, instead of the photon transverse momentum. This affects the expected signal yield by 4% (photon reconstruction efficiency) and 2% (photon PID efficiency). The uncertainties related to the photon energy scale and resolution affect the expected signal yield by 1% and 2%, respectively. The uncertainty due to imperfect knowledge of the photon angular resolution results in a 2% shift of the signal yield.

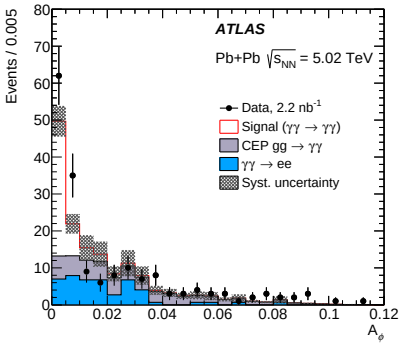

Figure 2: The diphoton acoplanarity distribution for events satisfying the signal region selection, but before applying the $Aco < 0.01$ requirement [2]. Data are shown as points with statistical error bars, while the histograms represent the expected signal and background levels. The CEP $gg \to \gamma\gamma$ background is normalised in the $Aco > 0.01$ control region.

The uncertainty due to the choice of signal MC generator is estimated by using an alternative signal MC sample. This affects the signal yield by 1% which is taken as a systematic uncertainty. The uncertainty due to the limited signal MC sample size is 1%. The uncertainty in the integrated luminosity of the data sample is 3.2%.

The uncertainty in the background yield is dominated by the uncertainty in the $\gamma\gamma \to ee$ background. This has a 6% impact on the estimated integrated fiducial cross section, and is a dominant source of systematic uncertainty.

5. Results

The measured integrated fiducial cross section is $\sigma_{\text{fid}} = 120 \pm 17\,(\text{stat.}) \pm 13\,(\text{syst.}) \pm 4\,(\text{lumi.})$ nb, which can be compared with the predicted values of 80 ± 8 nb from Ref. [8] and 78 ± 8 nb from the SuperChic v3.0 MC generator [9]. The data-to-theory ratios are 1.50 ± 0.32 and 1.54 ± 0.32, respectively.

Differential fiducial cross sections as a function of diphoton invariant mass, diphoton absolute rapidity, average photon transverse momentum and diphoton $|\cos\theta^*|$ are shown in Figure 3. They are compared with the predictions from SuperChic v3.0, which provide a fair description of the data, except for the overall normalisation differences. For nearly all variables and bins the total uncertainties in the cross-section measurements are dominated by statistical uncertainties, ranging from 25% to 75%.

The measured diphoton invariant mass spectrum is used to search for $\gamma\gamma \to a \to \gamma\gamma$ process, where a denotes the ALP. The SM LbyL, $\gamma\gamma \to ee$ and CEP $gg \to \gamma\gamma$ processes are considered as backgrounds. Events simulated with STARlight v2.0 [10], which implements the ALP couplings as described in Ref. [1], for various ALP masses between 5 GeV and 100 GeV are used to build an analytical model of the ALP signal, interpolating between the simulated mass points. In every analysis bin a cut-and-count analysis is performed to estimate the expected numbers of background and signal events. The bin-width is chosen to include at least 80% of a reconstructed ALP signal peak within a given bin and ranges from 2 GeV to 20 GeV.

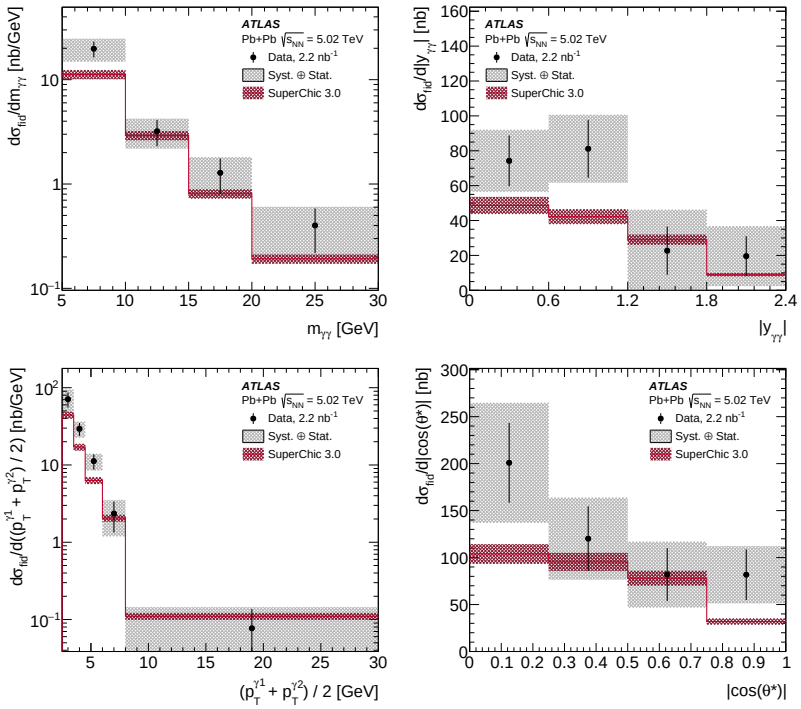

Figure 3: Measured differential fiducial cross sections of $\gamma\gamma \to \gamma\gamma$ production in Pb+Pb collisions at $\sqrt{s_{\mathrm{NN}}} = 5.02$ TeV for four observables (from left to right and top to bottom): diphoton invariant mass, diphoton absolute rapidity, average photon transverse momentum and diphoton $|\cos(\theta^*)|$ [2]. The measured cross-section values are shown as points with error bars giving the statistical uncertainty and grey bands indicating the size of the total uncertainty. The results are compared with the prediction from the SuperChic v3.0 MC generator (solid line) with bands denoting the theoretical uncertainty.

Since no significant deviation from the background-only hypothesis is observed, the result is then used to estimate the upper limit on the ALP production at 95% confidence level (CL). Assuming a 100% ALP decay branching fraction into photons, the derived constraints on the ALP mass and its coupling to photons are compared in Figure 4 with those obtained from various experiments. The exclusion limits from this analysis are the strongest so far for the mass range of $6 < m_a < 100$ GeV.

6. Summary

A measurement of the $\gamma\gamma \to \gamma\gamma$ scattering process in quasi-real photon interactions from ultra-peripheral Pb+Pb collisions at $\sqrt{s_{\mathrm{NN}}} = 5.02$ TeV by the ATLAS experiment at the LHC, is presented. The measurement is based on the full Run 2 data set.

Integrated and differential fiducial cross sections are measured as a function of several properties of the final-state photons and are compared with Standard Model theory predictions. All measured cross sections are consistent within 2 standard deviations with the predictions.

The measured diphoton invariant mass distribution is used to search for axion-like particles and set new exclusion limits on their production. These results provide, to this date, the most stringent

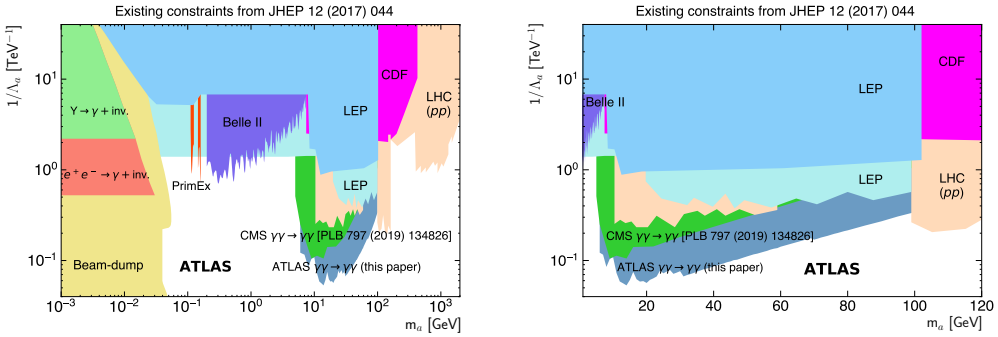

Figure 4: Compilation of exclusion limits at 95% CL in the ALP–photon coupling ($1/\Lambda_a$) versus ALP mass (m_a) plane obtained by different experiments [2]. The existing limits are compared with the limits extracted from this measurement. The exclusion limits labelled "LHC (pp)" are based on pp collision data from ATLAS and CMS. All measurements assume a 100% ALP decay branching fraction into photons. The plot on the right is a zoomed-in version covering the range $1 < m_a < 120$ GeV.

constraints in the search for ALP signals in the mass range of $6 < m_a < 100$ GeV.

7. Acknowledgements

The project is co-financed by the Polish National Agency for Academic Exchange within Polish Returns Programme, Grant No. PPN/PPO/2020/1/00002/U/00001.

References

[1] S. Knapen, T. Lin, H. K. Lou and T. Melia, Phys. Rev. Lett. **118**, no.17, 171801 (2017).

[2] ATLAS Collaboration, JHEP **03**, 243 (2021).

[3] D. d'Enterria and G. G. da Silveira, Phys. Rev. Lett. **111**, 080405 (2013) [erratum: Phys. Rev. Lett. **116**, no.12, 129901 (2016)].

[4] ATLAS Collaboration, JINST **3** (2008), S08003.

[5] ATLAS Collaboration, Nature Phys. **13** (2017) no.9, 852-858.

[6] CMS Collaboration, Phys. Lett. B **797**, 134826 (2019).

[7] ATLAS Collaboration, Phys. Rev. Lett. **123**, no.5, 052001 (2019).

[8] M. Kłusek-Gawenda, P. Lebiedowicz and A. Szczurek, Phys. Rev. C **93**, no.4, 044907 (2016).

[9] L. A. Harland-Lang, V. A. Khoze and M. G. Ryskin, Eur. Phys. J. C **79**, no.1, 39 (2019).

[10] S. R. Klein, J. Nystrand, J. Seger, Y. Gorbunov and J. Butterworth, Comput. Phys. Commun. **212**, 258-268 (2017).